

Measurement of the starspots temperature on HATS-2

Fanlin Meng¹, Yifan Li^{2,5}, Ziao Zhou³, Yi Zhang⁴

¹Department of Physics and Astronomy, Michigan State University, East Lansing, MI 48824, USA

²Department of Physics, Jilin University, Changchun, 130012, China

³Tsinglan School, Dongguan, 523808, China

⁴Department of Physics, Pennsylvania State University, State College, PA 16802, USA

⁵liyf1118@mails.jlu.edu.cn

Abstract. The study of exoplanets is a significant branch of astrophysics. And the study of exoplanets could always reveal some properties of host stars. In this work, the latest data from Transiting Exoplanet Survey Satellite was used to study the transiting exoplanet, HATS-2b. The study of HATS-2b revealed an interesting thing: its host star, HATS-2 shows noticeable starspot activity. The discovery and analysis of six starspots in 2019 to 2023 is presented in this paper. Numerous anomalies were present in transit light curves of HATS-2, that we interpreted as the planet, HATS-2b occulting dark starspots. This work used a new method by creating a simplified model which is based on the transit method to measure the temperature of starspots, which means that in the future, some researchers who are looking to confirm the existence of starspots on the photosphere of certain stars can use the method in this paper first to measure the approximate temperature of objects they observe in order to investigate whether observed objects are indeed starspots. The work calculated the temperature of six spots, which was determined by applying Planck's law of radiation: 3477 ± 40 K, 3788 ± 24.5 K, 3881 ± 33.5 K, 3783 ± 117 K, 3256 ± 130 K, 4240 ± 18 K. Additionally, the work refined the planetary parameters of HATS-2b with using the latest data and compared the recent starspot activity with data from literature.

Keywords: Exoplanets, Transit, Starspots, HATS-2.

1. Introduction

Starspots are dark and cool regions that appear on star's photosphere, which are formed from interaction of the stellar magnetic field lines and turbulent convection. When magnetic field lines are disturbed and strong magnetic fields form, near surface convection is inhibited, lowering the temperature of surrounding area and creating a dark starspot [1]. In previous studies of eclipsing planets, researchers have found that a planet passing over a starspot on the host star can potentially increase the flux received [2, 3]. This is due to the fact that starspots are often cooler than the rest of the photosphere, which emits less flux than surrounding regions. When planets transit across starspots, less light is blocked compared to transiting unspotted areas of the photosphere, thus affecting the light curve of a star by creating an anomalous brightening in the middle of a transit [4].

However, an anomaly in flux may not only be the result of a starspot, but also other phenomena such as a third body, measurement errors, star pulsation, etc [5]. In the first case, there has to be another large enough body to coincidentally pass the transiting planet, so they overlap and less light is blocked, while a star pulsation depends on the star type.

HATS-2 is a K-type dwarf star with an effective surface temperature $4985^{+125.444}_{-121.586}$ K and it is found to have observable starspots by a HATSouth survey in 2013 [6, 7]. The mass of HATS-2 is $0.882 \pm 0.037 M_{\text{sun}}$, while HATS-2b, the transiting planet of HATS-2 system is a hot Jupiter of mass $1.345 \pm 0.150 M_J$ and orbital period $1.35413371 \pm 0.00000026$ Earth days [7, 8]. In the special case of HATS-2b, it is possible to observe statistically significant bumps while the planet is eclipsing, and properties related to the starspot can be found. For instance, Mohler-Fischer et al. measured the temperatures and sizes for two determined starspots they found, by fitting the anomalous transit to obtain the spot size and spot contrast f_i (the ratio of the surface brightness of the spot to that of the surrounding photosphere) and finally applying the Equation (1) of Silva to calculate starspots temperature [4, 7]. In Equation (1), h is the Planck constant, T_e is the effective temperature of the star and T_0 is the starspot temperature.

$$f_i = \frac{\exp(h\nu/k_B T_e) - 1}{\exp(h\nu/k_B T_0) - 1} \quad (1)$$

The study of starspots are significant as they can be applied to measure other important parameters. As an example, Sanchis-Ojeda et al. developed a method to find the obliquity of a star between the spinning axis and orbital plane of the planet by building geometric models and solving for stellar geometry [9]. In this way, they were able to measure the obliquity, active latitudes for starspots, and misalignment between the spin orbits of a particular star and planet.

The work updated the planet parameters of HATS-2b with public datasets from NASA Transiting Exoplanet Survey Satellite (TESS), considering the star spot anomalies [10]. So far, there is not any work on HATS-2 that uses TESS data with considering starspots, so all sectors spanning from 2019 to 2023 should be new to the field. In addition, the temperature for a total of six starspots was measured, two for each Sector, and analysed the star spot activities in these few years was analysed in this work.

2. Observations

We obtained three light curves for HATS-2 from Sector 10 (2019) , 36 (2021) , and 63 (2023) in TESS data, with an exposure time of 120s. TESS uses a red-optical bandpass with a wavelength between 600nm and 1000nm in which Mohler-Fischer et al. observed bump in transit light curves so that the TESS data could be analysed directly [7, 10].

Firstly, a normalisation was done on flux by dividing the TESS flux data with the median of all out of transit fluxes. By doing so, it is possible to set the flux at around 1.0 and the original flux unit (electrons per second) is not needed to be considered. Secondly, we sorted the time with the orbital period provided in previous studies and folded all orbits of transits into one single transit [8]. Thirdly, each epoch in each sector is plotted respectively and it is easy to notice anomalies in transit durations. There was a small increase in flux in more than a third of the orbits, which was interpreted as planets crossing irregularities on the stellar photosphere. The epochs that have substantial anomalies were extracted, two for each sector. One of light curves of HATS-2 is shown in Figure 1 in blue errorbars along with the fitted model which will be explained in Section 3. And the folded light curve of HATS-2 (Sector 63) is shown in Figure 2.

3. Methods

3.1. Excluding other possibilities of anomalies

For the anomalies discovered, there are several probabilities of why it occurs but they were narrowed down to one. From analysis of Mohler-Fischer et al. by using method of Hartman et al., the idea of a third body crossing was rejected as the odds of that is proven to be small [7, 11]. Pulses are not the reason as HATS-2 is shown to be a K-type dwarf star that do not pulsate, which left us with only two possibilities left [7]. Previous studies from Mohler-Fischer et al. had also found anomalies with the HATSouth telescope, different from what was used in this work so technical issues should not be the case, and they concluded it to starspots, giving us a clue that the anomaly may be due to starspots [7]. Additionally, there are periodic background patterns in out of transit areas that might be a result from

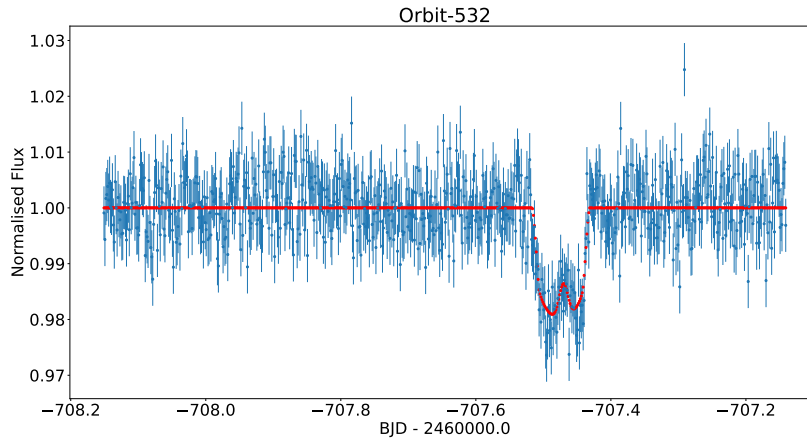


Figure 1: [Owner-draw] One of light curves of HATS-2 resulting from the fit described in Section 3. The red line shows the fit model.

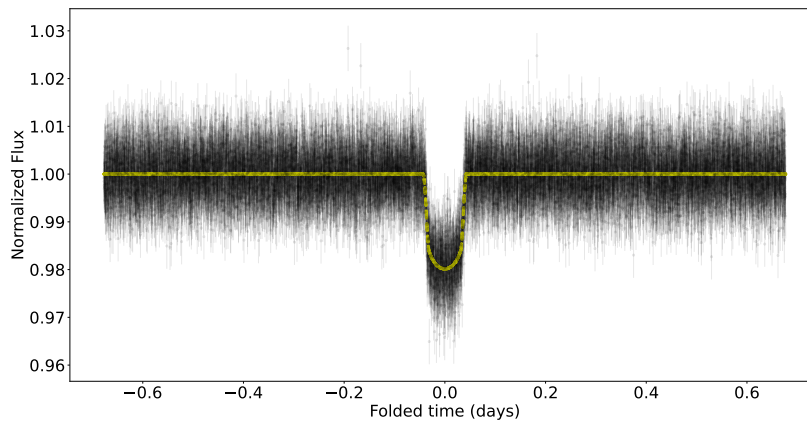


Figure 2: [Owner-draw] Here is the folded light curve of HATS-2 resulting from the global fit. The yellow line shows the fit model.

starspots affecting the luminosity when the star rotates. Therefore it was interpreted as a consequence of planets occulting starspots on the stellar photosphere.

3.2. Model building

Because we could not know the actual shape or size of starspots from TESS data, the model was built with a few assumptions:

- 1.The starspots are all perfect circles.
- 2.During the transit, the planet can block the starspot that showed in the data completely. There is no partial block.

When processing light curves with star spot anomalies, it is essential to model the transit together with the anomaly or else the system parameters calculated may be biased. This work model the normal transit part first with the basic geometry of eclipses then creating another model for the anomaly. A total

of nine parameters is used, listed below:

- 1.time of conjunction (tc)
- 2.orbital period of planet (p)
- 3.ratio of radii (r_p/r_s)
- 4.linear limb darkening coefficient (u)
- 5.radius of orbit/ radius of star (a)
- 6.impact parameter (b, $a \cos(I)/r_s$)
- 7.interval from anomaly midpoint to transit midpoint (Δtc)
- 8.amplitude of bump (ampl)
- 9.standard deviation of Gaussian bump in days (width)

The first six is for the transit [12]. In particular, parameter r_p is the radius of the planet, r_s is the radius of the host star and I is orbital inclination [12]. By building a 3D coordinate system, it is able to find that the x-axis (side view) is

$$X(t) = a \sin \Phi(t) \quad (2)$$

and y-axis (top view) is

$$Y(t) = a \cos I \cos \Phi(t), \quad (3)$$

where Φ is the orbital phase and I is orbital inclination. Thus, the separation between star and planet is

$$\sqrt{X^2 + Y^2} \quad (4)$$

It is then possible to use the limb darkened transit model from Mandel, K. and Agol, E. to find the loss of flux due to transit, and a linear limb darkening coefficient is more suited to the model in this work [13]. A Gaussian function is applied to simulate the anomalous bump, using the last three parameters:

$$f_{\text{bump}} = \text{ampl} * e^{(-0.5 * (t - (tc + \Delta tc) / \text{width})^2)} \quad (5)$$

The minimum for amplitude is zero, as the work do not expect a decrease in flux for starspots. We also limit the delta tc to be no longer than half the transit duration, so the bump does not occur in out of transit areas.

3.3. Fitting data

In the work, a first attempt at fitting an entire sector as a folded transit was made, setting all nine variables as free parameters and their guesses as data from previous researches [8]. An initial result was obtained for the nine parameters. The parameter tc and period that the work obtained by using the latest TESS data is shown in Table 1. The starspots parameters are different from transit parameters. The starspots parameters are rough and have a large deviation if used for single epochs, but they gave an insight to the order of magnitude of the parameters. It will improve the initial guesses for the LM-fit model. Then selected epochs were fitted one by one, as the parameter values can be very different with different epochs. In the work, the six transit parameters were invariable; they were set to the values of the initial fitting results. The other three was let to vary and the initial guesses was adjusted until the fit is reasonable. Fitted curves are shown in red in Figure 3 and the results for the parameter amplitude are in Table 2.

3.4. Obtaining $\Delta F/F_0$, uncertainty and calculating

Based on our assumption, the star and starspots were considered as black body. The Planck's Law illustrates the relation between radiance and radiation frequency of black body radiation which is emitted by black bodies at different temperatures. So the Planck's Law could be used to calculate the temperature of starspots. According to the Planck's Law

$$B(\nu) = \frac{2h\nu^3}{c^2} \frac{1}{e^{\frac{h\nu}{k_B T}} - 1} \quad (6)$$

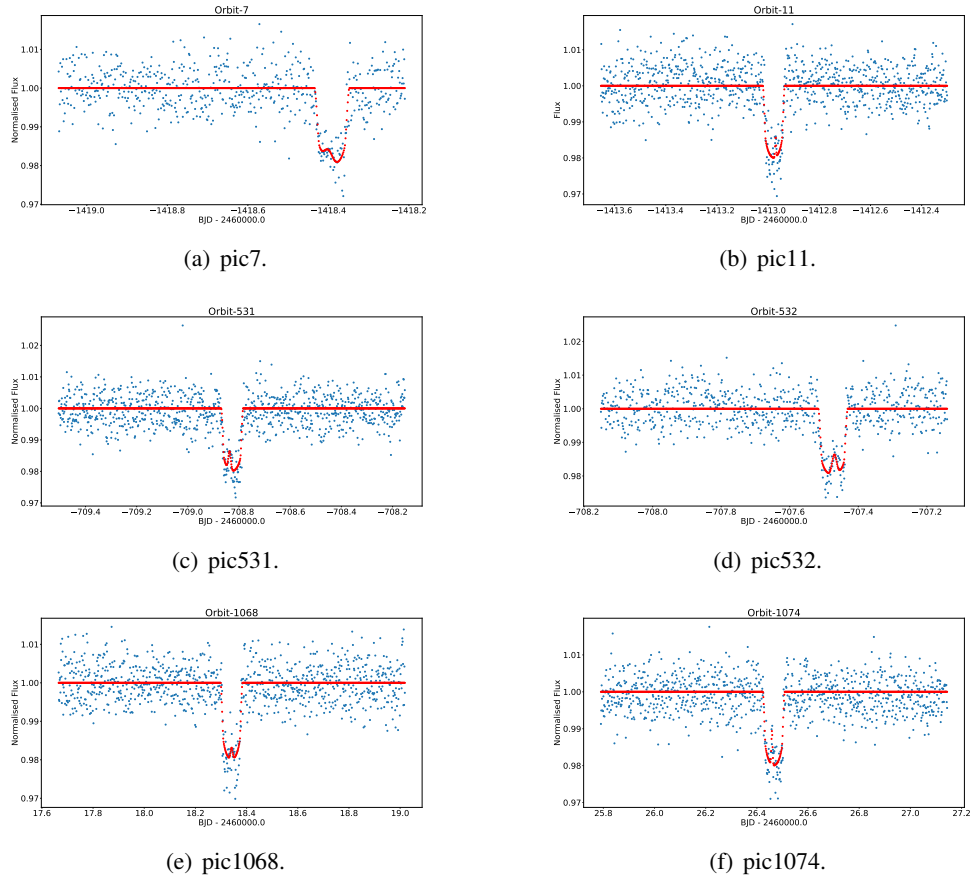


Figure 3: [Owner-draw] Here is six fitted curves, red dots show the fit model.

Table 1: Transit parameters [Owner-draw]

Parameter	Value
tc	$2460015.63399 \pm 0.00038$ days
period	1.35411689 ± 0.000038 days

NOTES. The two transit parameters were obtained by using the latest TESS data.

Table 2: Ampl values [Owner-draw]

Orbit number	ampl	unc
7	0.00401	0.00168
11	0.00569	0.00410
531	0.00594	0.00240
532	0.00631	0.00213
1068	0.00309	0.00254
1074	0.00918	0.00352

NOTES. This table shows the parameter amplitude which indicates the change of flux caused by starspots.

in the Equation (6), h is the Planck constant, B is the radiance and ν is the radiation frequency, we could integrate the Equation (6) over different frequencies so that the intensity of black body radiation with the constant T could be obtained. For this work, the radiation frequency is the frequency of the TESS's instrument which could be obtained from Ricker et al. [10]. And the flux obtained from TESS represents the intensity because $I = F/\pi R^2$. In particular, I is intensity and F is flux. That means the value of $\Delta F/F_0$, which is the difference between the flux of starspot and star photosphere divided by the flux of photosphere could be used to obtain the value of the effective surface temperature of HATS-2 divided by the temperature of the starspot. The values of $\Delta F/F_0$ could be obtained from light curves and the values are shown in the Table 3. Since the flux, the radiation frequency and the effective surface temperature of HATS-2 has been obtained, the temperature of the starspot is the only unknown variable. Then an equation could be set up

$$\frac{T_{\text{spot}}^3 \int_{x_1(T)}^{x_2(T)} \frac{x^2}{e^x - 1} dx}{T_{\text{star}}^3 \int_{x_1(T)}^{x_2(T)} \frac{x^2}{e^x - 1} dx} = \frac{\Delta F}{F_0} \left(\frac{r_s}{r_p}\right)^2 \quad (7)$$

which is based on the Planck's law. In the Equation (7), T_{spot} is the temperature of the starspot, T_{star} is the effective surface temperature of HATS-2 and $x = \frac{h\nu}{k_B T}$. x_1 corresponds to $\nu = 600nm$ and x_2 corresponds to $\nu = 1000nm$ [10].

Table 3: $\Delta F/F_0$ values [Owner-draw]

Orbit number	$\Delta F/F_0$	unc
7	0.0035522	0.0004619
11	0.0055450	0.0001533
531	0.006125	0.0001851
532	0.0054701	0.0007196
1068	0.0025433	0.0005494
1074	0.0092813	0.0001039

NOTES. The value of ΔF is the change of flux caused by starspots.

Table 4: Temperature [Owner-draw]

Orbit number	T_{spot}
7	3477 ± 40 K
11	3788 ± 24.5 K
531	3881 ± 33.5 K
532	3783 ± 117 K
1068	3256 ± 130 K
1074	4240 ± 18 K

NOTES. The work used the latest stellar effective temperature which came from the research of [6] as the effective temperature of the unspotted photosphere. $T_{\text{star}} = 4985K$.

3.5. Uncertainty of T_{spot}

For the uncertainty of T_{spot} , at first the uncertainty of the ampl parameter from the fitting result was considered to be taken and calculate the T_{spot} of the upper bound and lower bound. Unfortunately,

for some epochs, the uncertainty given from fitting is too large to be used in the calculateion of T_{spot} . Instead, in this work the uncertainty was determined as follows. The ampl parameter is a factor for the shape of the Gaussian bump, and it represents the height of the Gaussian function's peak. The work define another difference in flux which was called ΔF to be the maximum value of the Guassian bump minus the minimum value of the transit curve. However, the maximum and minimum point do not have the same value for time, which means that there might be error when calculating ΔF . So an approximation was made. Because selected bumps selected were all close to tc, the approximation was made due to $\lim_{x \rightarrow 0} \frac{x}{1-x} = x$. This approximation assumed that each bump occurred at tc. And then the difference between the amplitude of Guassian and ΔF was measured, and such value was used as the uncertainty of ΔF . Adding or subtracting that uncertainty to ΔF and calculating the responding T_{spot} gives the T_{spot} with temperature range.

4. Results

Table 1 shows the planetary parameters time of conjunction and period this work obtained and Table 4 presents the measured temperatures of starspots. The temperature of the starspots measured in the work are within the theoretically expected range of 500-2000K cooler than 4985K, the effective temperature of the star, thus it would be safe to say that the bumps in the transit data are truly the result of the starspots. The temperatures have a relatively even distribution, with no particularly large or small values, further confirming the existence of starspots [14].

For the results in this work, starspots have a range of around 800-1800K cooler than the stellar photosphere. In previous research, Mohler-Fischer et al. found that the temperature of starspots in the star photosphere of HATS-2 were within the range about 400-900K cooler than the star photosphere [7]. However, their data of the two starspots were obtained using different frequency filters and one of them shows different temperatures in different wavelength ranges, namely they obtained a range of the same starspot's temperature is about 600-1700K cooler than the star photosphere, which is very close to the range in this work. According to this, the main reason why the results were so different from results of Mohler-Fischer et al. was obtaining data from different telescopes [7]. As this work only used TESS data to measure the temperature of starspots, light curves obtained by different filters which have different bandpass could not be analysed so that it would not be safe to assure whether some specific starspots affect light curves in specific wavelength ranges. Furthermore, the spectral response function of TESS is different from that of each filter Mohler-Fischer et al. used, which could be another possible reason [7, 10].

5. Discussion

5.1. Model and Fitting

When testing how reasonable the fitting is, the reduced chi-square of the fit of each epoch was be taken and compared with 1. A fixed uncertainty of the flux was set that is the same for all epochs, which is the numerical standard deviation of all flux values in out-of-transit part, assuming it to be the systemic fluctuation caused by unimportant factors.(This uncertainty is not to be confused with the uncertainty of the amplitude or the temperature of starspots mentioned earlier. It is only representing the background fluctuation present in the transit.) Then the residuals were calculated by dividing the difference of calculated flux and actual flux with the fixed uncertainty. This residual is prepared for the Minimizer and minimize function in LMfit, which returns the reduced chi-square. The results are presented in Table 5. It turns out that the reduced chi-squares for the fittings are relatively high; some are higher than 1. We tried several ways of limiting the maximum and minimum of parameters and setting some parameters not to vary, but the result was unsatisfying.

According to previous studies, many researches also faced the same problem of chi-square higher than 1, the expected value for a good fit [15, 16]. So we decide to adjust the fit until the chi-square is as low as possible, and select the two epochs from each sector with the lowest chi-squares (even if it is

Table 5: Reduced χ^2 [Owner-draw]

Orbit number	χ_{red}^2
7	0.95713
11	1.00086
531	1.03587
532	1.11219
1068	0.93349
1074	0.92878

NOTES. The Reduced χ^2 was calculated by using fitting results.

higher than 1.0) for further starspots analysis.

The main reason might be that the model in this work is crude. A simplified model was created, for example, which does not include situations where the planet only partially blocks the starspots or when starspots are not circles, which is not enough to fit very accurately on the real case. It could be improved if a quadratic limbed darkening coefficient is used and in reference to the PRISM and GEMC codes, a pixellation approach used to create the modelled star on a two-dimensional array in Cartesian coordinates, which means the model has to model all three (limb darkening, starspot, transit) geometrically on one stellar disc [17]. In addition, cases where starspots are partially blocked should also be added and considered. Nevertheless, the model in this work is advantageous in dealing with the anomaly. From literature, a lot of times the anomalous transit was modeled as a normal transit and the starspots are analyzed based on the residuals from the fitting, which can cause bias in measurements of the parameters [1, 9, 17, 18]. This problem was prevented in this work as the anomaly and the transit was modeled separately in the work, allowing a greater accuracy in the fit. Other reasons for the high chi-square might be associated with the systemic uncertainty which was set to be fixed, the initial guesses, etc. For the same reason, systemic uncertainties of the model in this work are not considered in the calculation. The uncertainty of the starspot temperatures provided before is only a result of fitting.

To improve the accuracy of the temperature measurements even more, multiple filters should be used from another telescope. The advantage of multi-filter is that the starspot can be measured from several aspects, and taking the average of those can reduce the uncertainty. Furthermore, it helps to prove that an anomaly is truly a starspot event, as a starspot would occur in all filters but a noise would appear different in different filters.

5.2. Future possible directions

From the results in this work, it would be safe to say that there are some starspot activities on HATS-2. And the temperature of some starspots was measured, and each of them are within the range about 800-1800K cooler than the star photosphere.

The six epochs chosen are only a fraction of around 25 more anomalous epochs, while the amount is consistent during the three years. The lifespan of starspots on HATS-2 is predicted to be about 130 days, which means that the six starspots are likely to be entirely different spots and the star is continuously producing a significant number of starspots every year [7]. From the number of anomalies observed in this work, it is evident that HATS-2 is a star that has intense starspot activities, indicating that it might have a very turbulent and chaotic magnetic field and stellar phenomena like solar flare are common. There is a chance that this turbulent magnetic field might mean that HATS-2 is a young star, according to an age-magnetic study from Vidotto et al. [19]. If HATS-2 is indeed a young star, the surface temperature of the stellar photosphere can be significantly affected by the starspots, which might provide a direction for future studies on HATS-2 [20]. At the same time, anomalies are present in more than a third of

the data collected from TESS and the separation between starspots in one sector is within 130 days, providing a good condition for stellar obliquity measurements. Furthermore, although this work only have data from three sectors, the data showed that Sector 10 (2019) seems to have less active starspot activity than other two sectors, namely less anomalies were seen in the light curves, and TESS observed the most anomalies in Sector 36 (2021), indicating that we might be able to measure the period of the starspot activity. Thus there was an assumption that starspots of HATS-2 might be in an active state in 2021 and maybe the period of the starspot activity of HATS-2 is coincidentally 5 years (from 2018 to 2023). This is only a guess based on the three sectors' data and the assumption could not be confirmed because the data is not enough to accomplish that. However, determining the period of the starspot activity on HATS-2 might be possible if more data about HATS-2 within a long period of time could be available, and this is also an interesting topic to investigate in the future.

6. Conclusions

Starspots analysis, such as the measurement of starspot temperatures, is an important field of study as they are the fundament of many other findings, ranging from stellar obliquities to exoplanet atmospheres. In this work, HATS-2's light curves from TESS, data that has never been used before was obtained to study this star, and a simplified model was created, which allows the fitting of anomalies and transits to occur at the same time, ensuring less uncertainty. Temperatures of six more starspots with a larger time interval is presented, while only two was measured before. In future mission, it will be possible to analyze HATS-2's starspots using multi-filters to obtain a more accurate temperature result and more data will allow more discoveries on the stellar magnetic activity.

Acknowledgment

All authors contributed equally to this work and should be considered co-first authors.

References

- [1] Ballerini P, Micela G, Lanza A F and Pagano I 2012 *Astronomy and Astrophysics* 539 A140 (*Preprint* 1201.3514)
- [2] Rabus M, Alonso R, Belmonte J A, Deeg H J, Gilliland R L, Almenara J M, Brown T M, Charbonneau D and Mandushev G 2009 *Astronomy and Astrophysics* 494 391–397 (*Preprint* 0812.1799)
- [3] Pont F, Gilliland R L, Moutou C, Charbonneau D, Bouchy F, Brown T M, Mayor M, Queloz D, Santos N and Udry S 2007 *Astronomy and Astrophysics* 476 1347–1355 (*Preprint* 0707.1940)
- [4] Silva A V R 2003 *The Astrophysical Journal* 585 L147–L150
- [5] Watson R D 1988 *Astrophysics and Space Science* 140 255–290
- [6] Stassun K G, Oelkers R J, Paegert M, Torres G, Pepper J, De Lee N, Collins K, Latham D W, Muirhead P S, Chittidi J, Rojas-Ayala B, Fleming S W, Rose M E, Tenenbaum P, Ting E B, Kane S R, Barclay T, Bean J L, Brassuer C E, Charbonneau D, Ge J, Lissauer J J, Mann A W, McLean B, Mullally S, Narita N, Plavchan P, Ricker G R, Sasselov D, Seager S, Sharma S, Shiao B, Sozzetti A, Stello D, Vanderspek R, Wallace G and Winn J N 2019 *The Astronomical Journal* 158 138 (*Preprint* 1905.10694)
- [7] Mohler-Fischer M, Mancini L, Hartman J D, Bakos G Á, Penev K, Bayliss D, Jordán A, Csubry Z, Zhou G, Rabus M, Nikolov N, Brahm R, Espinoza N, Buchhave L A, Béky B, Suc V, Csák B, Henning T, Wright D J, Tinney C G, Addison B C, Schmidt B, Noyes R W, Papp I, Lázár J, Sári P and Conroy P 2013 *Astronomy and Astrophysics* 558 A55 (*Preprint* 1304.2140)
- [8] Ivshina E S and Winn J N 2022 *The Astrophysical Journal Supplement Series* 259 62 (*Preprint* 2202.03401)

- [9] Sanchis-Ojeda R, Winn J N, Holman M J, Carter J A, Osip D J and Fuentes C I 2011 *The Astrophysical Journal* 733 127 (Preprint 1103.4859)
- [10] Ricker G R, Winn J N, Vanderspek R, Latham D W, Bakos G Á, Bean J L, Berta-Thompson Z K, Brown T M, Buchhave L, Butler N R, Butler R P, Chaplin W J, Charbonneau D, Christensen-Dalsgaard J, Clampin M, Deming D, Doty J, De Lee N, Dressing C, Dunham E W, Endl M, Fressin F, Ge J, Henning T, Holman M J, Howard A W, Ida S, Jenkins J M, Jernigan G, Johnson J A, Kaltenegger L, Kawai N, Kjeldsen H, Laughlin G, Levine A M, Lin D, Lissauer J J, MacQueen P, Marcy G, McCullough P R, Morton T D, Narita N, Paegert M, Palte E, Pepe F, Pepper J, Quirrenbach A, Rinehart S A, Sasselov D, Sato B, Seager S, Sozzetti A, Stassun K G, Sullivan P, Szentgyorgyi A, Torres G, Udry S and Villaseñor J 2015 *Journal of Astronomical Telescopes, Instruments, and Systems* 1 014003
- [11] Hartman J D, Bakos G Á, Torres G, Latham D W, Kovács G, Béky B, Quinn S N, Mazeh T, Shporer A, Marcy G W, Howard A W, Fischer D A, Johnson J A, Esquerdo G A, Noyes R W, Sasselov D D, Stefanik R P, Fernandez J M, Szklenár T, Lázár J, Papp I and Sári P 2011 *The Astrophysical Journal* 742 59 (Preprint 1106.1212)
- [12] Winn J N 2010 *Exoplanets* ed Seager S pp 55–77
- [13] Mandel K and Agol E 2002 *The Astrophysical Journal* 580 L171–L175 (Preprint astro-ph/0210099)
- [14] Berdyugina S V 2005 *Living Reviews in Solar Physics* 2 8
- [15] Southworth J, Tregloan-Reed J, Andersen M I, Calchi Novati S, Ciceri S, Colque J P, D’Ago G, Dominik M, Evans D F, Gu S H, Herrera-Cordova A, Hinse T C, Jørgensen U G, Juncher D, Kuffmeier M, Mancini L, Peixinho N, Popovas A, Rabus M, Skottfelt J, Tronsgaard R, Unda-Sanzana E, Wang X B, Wertz O, Alsubai K A, Andersen J M, Bozza V, Bramich D M, Burgdorf M, Damerdjy Y, Diehl C, Elyiv A, Figuera Jaimes R, Haugbølle T, Hundertmark M, Kains N, Kerins E, Korhonen H, Liebig C, Mathiasen M, Penny M T, Rahvar S, Scarpetta G, Schmidt R W, Snodgrass C, Starkey D, Surdej J, Vilela C, von Essen C and Wang Y 2016 *Monthly Notices of the Royal Astronomical Society* 457 4205–4217 (Preprint 1512.05549)
- [16] Baştürk Ö, Esmer E M, Yalçinkaya S, Torun Ş, Mancini L, Helweh F, Karamanlı E, Southworth J, Aliş S, Wünsche A, Tezcan F, Aladağ Y, Aksaker N, Tunç E, Davoudi F, Fişek S, Bretton M, Evans D F, Yeşilyaprak C, Yılmaz M, Tezcan C T and Yelkenci K 2022 *Monthly Notices of the Royal Astronomical Society* 512 2062–2081 (Preprint 2203.00299)
- [17] Tregloan-Reed J, Southworth J and Tappert C 2013 *Monthly Notices of the Royal Astronomical Society* 428 3671–3679 (Preprint 1211.0864)
- [18] Maciejewski G, Raetz S, Nettelmann N, Seeliger M, Adam C, Nowak G and Neuhäuser R 2011 *Astronomy and Astrophysics* 535 A7 (Preprint 1109.4749)
- [19] Vidotto A A, Gregory S G, Jardine M, Donati J F, Petit P, Morin J, Folsom C P, Bouvier J, Cameron A C, Hussain G, Marsden S, Waite I A, Fares R, Jeffers S and do Nascimento J D 2014 *Monthly Notices of the Royal Astronomical Society* 441 2361–2374 (Preprint 1404.2733)
- [20] Flores C, Connelley M S, Reipurth B and Duchêne G 2022 *The Astrophysical Journal* 925 21 (Preprint 2111.03957)